

## **AUTOMATIC DETERMINATION OF PID CONTROLLER PARAMETERS BY USING SIMULINK AND ITS JUSTIFICATION IN SIMULATING VEHICLE ACTIVE SUSPENSION SYSTEM**

**Jasmin Sehovic, B.Sc.\***

**Boran Pikula, Ph.D.\*\***

---

### **Abstract**

This paper will present the development of oscillatory models of active suspension system. It is accomplished by modifying oscillatory models of passive suspension system by introducing active force into the system presented by PID controller. One-dimensional, two-dimensional and three-dimensional vehicle oscillatory models with active suspension system are formed. Adjustment of PID controller parameters was conducted automatically by using Simulink programme. Analysis and comparison of individual oscillatory parameters for one-dimensional, two-dimensional and three-dimensional oscillatory model of passive and active suspension system were also completed. The obtained results of vertical movement of sprung mass (vehicle body) and unsprung mass (wheels), as well as sprung mass angle rotation around  $x$  and  $y$  axes of a vehicle justify the use of PID controller for simulating the behaviour of a vehicle active suspension system.

**Key words:** PID controller, Simulink, active suspension, vertical oscillations, sprung mass, unsprung mass

---

**\*PhD candidate, Faculty of Mechanical Engineering Sarajevo, University of Sarajevo, Bosnia and Herzegovina**

**\*\*Associate Professor, Faculty of mechanical engineering Sarajevo, University of Sarajevo, Bosnia and Herzegovina**

## 1. Introduction

Movement of a vehicle on the road is always accompanied by the influence of external and internal forces, which are transferred to the vehicle through wheels. As the vehicle body leans on the wheels by means of suspension system, this causes the occurrence of oscillation of the vehicle body in direction of the vertical axis of the vehicle and around the axis of the vehicle. Suspension system is an important system whose role is to provide comfort and safety to passengers and cargoes for all road vehicles. These two parameters are always in negative conjunction with each other, which means that a compromise between safety in the movement of vehicles and passenger comfort must be created. It is possible to influence these two elements through damping characteristics and stiffness elements of suspension system for classic (passive) suspension systems. [1, 2].

However, during vehicle movement and particularly under the influence of inertial forces in the longitudinal motion, as well as the effects of centrifugal force of a vehicle in a curve, significant oscillations of the vehicle sprung mass occur. The aforementioned swinging of a sprung mass as a result of the influence of the gyroscopic moment additionally undermines stability of a vehicle.

Due to this, recently an active research has been developed on the introduction of semi-active and active suspension for modern passenger vehicles, which aim to minimize or even completely eliminate the swinging of a sprung mass. In order to achieve this task, certain elements in suspension system must have variable parameters of damping and stiffness [3]. Oscillatory vehicle models are introduced to conduct research on oscillatory behaviour of vehicles in the analysis of performance of suspension systems [4]. Oscillatory models can be solved and analysed by using any of the MBS (Multi Body Simulation) programmes, or numerically by using MATLAB or by simulation using Simulink. One of the most commonly used software for analysis of these models is Simulink within package programme Matlab [5]. Modelling of active suspension system in Simulink is normally reduced to optimization by PID (Proportional Integral Derivative) controller through analysis of  $\frac{1}{4}$  vehicle model [6]. The general equation of this controller is given by equation (1), and the general scheme of the controller is shown in Figure 1 [7].

$$x(t) = K_p \left[ u(t) + \frac{1}{T_i} \int_0^t u(t) + T_d \frac{du}{dt} \right] \quad (1)$$

The most important segment in optimizing PID controller is determining its parameters  $K_p$ ,  $K_i$  and  $K_d$ . In the example shown in [8] Ziegler-Nichols method, which is used to determine these parameters, was explained. However, Simulink provides the possibility of automatically determining parameters and in this paper these parameters will be automatically determined using the block of PID controller in Simulink programme. Some parameters of oscillatory behavior of the sprung mass (body) and the unsprung mass (wheel) in the case of passive and active suspension system will be analysed and compared. The analysis will be carried out for cases  $\frac{1}{4}$ ,  $\frac{1}{2}$  and a full vehicle model.

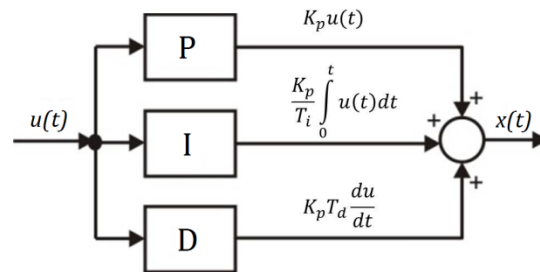


Figure 1. Block structure of PID controller

## 2. Forces and moments acting on a vehicle

The equations of vehicle motion in the study of vehicle dynamics are usually represented by a system of equations in the coordinate system (Txyz) related to the vehicle in the center of gravity of the vehicle T. The  $x$ -axis is longitudinal and it is directed at the vehicle, the  $y$ -axis is perpendicular to the lateral vehicle plane, and the  $z$ -axis is perpendicular to the horizontal vehicle plane. The resultant forces and moments are shown in Figure 2. in the directions  $x$ ,  $y$  and  $z$ -axes which can act on a vehicle in general case of vehicle movement.

The general equations for resulting force and moment which act on a vehicle are presented by the following equation:

$$\begin{aligned} F &= F_x \vec{i} + F_y \vec{j} + F_z \vec{k} \\ M &= M_x \vec{i} + M_y \vec{j} + M_z \vec{k} \end{aligned} \quad (2)$$

Whereas

$F_x$  – resulting force acting on a vehicle in the direction of x-axis,

$F_y$  – resulting force acting on a vehicle in the direction of y-axis,

$F_z$  – resulting force acting on a vehicle in the direction of z-axis,

$M_x$  – resulting moment acting on a vehicle around x-axis,

$M_y$  – resulting moment acting on a vehicle around y-axis,

$M_z$  – resulting moment acting on a vehicle around z-axis.

In order to form the oscillatory model, the effect of all the forces is neglected, apart from the vertical one. Next, the oscillatory models of vehicles for the analysis of active suspension systems are presented.

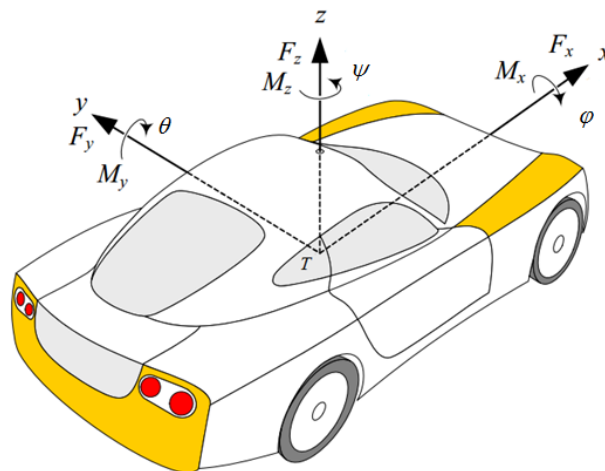


Figure 2. *Vehicle with coordinate system*

### 3. Vehicle oscillatory models

#### 3.1. One-dimensional vehicle model

The most commonly used model of vehicles during the analysis of oscillatory behaviour on vehicles, especially passenger vehicles, is one-dimensional model with two masses (sprung mass  $m_v$  and unsprung mass  $m_T$ ), as shown in Figure 3. This model is often called  $\frac{1}{4}$  of vehicle model.

Figure 3. shows that the influence of damping in the tire is ignored for this analysis.

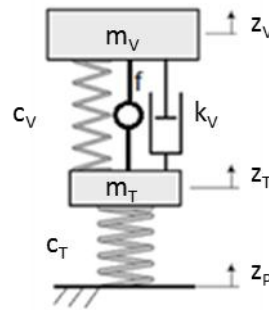


Figure 3. *One-dimensional oscillatory model with two masses*

Equations of oscillation of sprung mass – the vehicle body ( $m_V$ ) and unsprung mass - wheels ( $m_T$ ) in the direction of  $z$ -axis is presented next. Equation of oscillation of sprung mass in the  $z$ -axis direction is as follows:

$$m_V \cdot \frac{d^2 z_V}{dt^2} + k_V \left( \frac{dz_V}{dt} - \frac{dz_T}{dt} \right) + c_V (z_V - z_T) - f = 0 \quad (3)$$

Equation of oscillation of unsprung mass in  $z$ -axis direction is as follows:

$$m_T \cdot \frac{d^2 z_T}{dt^2} + k_V \left( \frac{dz_T}{dt} - \frac{dz_V}{dt} \right) + c_V (z_T - z_V) + c_T (z_T - z_P) + f = 0 \quad (4)$$

In the equations (3) and (4) parameter  $f$  presents the force which is used by active suspension system to perform settling and damping of oscillations of sprung mass of vehicles ( $m_V$ ).

### 3.2. Two-dimensional vehicle model

This model is also called the model of half of a vehicle. Two-dimensional model replaces the vehicle more precisely because it takes into consideration suspension of sprung mass over two or more axles. Based on this model it is possible to analyse vertical as well as oscillations around the axis perpendicular to longitudinal plane of the analysed vehicle oscillatory model ( $m_V$ ).

Model which replaces the vehicle during the analysis of oscillatory behaviour of a vehicle is shown in Figure 4.

Figure 4. shows sprung mass ( $m_V$ ), front axle unsprung mass ( $m_{TP}$ ), rear axle unsprung mass ( $m_{TZ}$ ). It can also be seen that sprung mass has an inertia moment around  $y$ -axis (axis

perpendicular to longitudinal plane) marked as  $J_Y$ . Active forces which perform settling down of vertical oscillations are marked as  $f_P$  and  $f_Z$ .

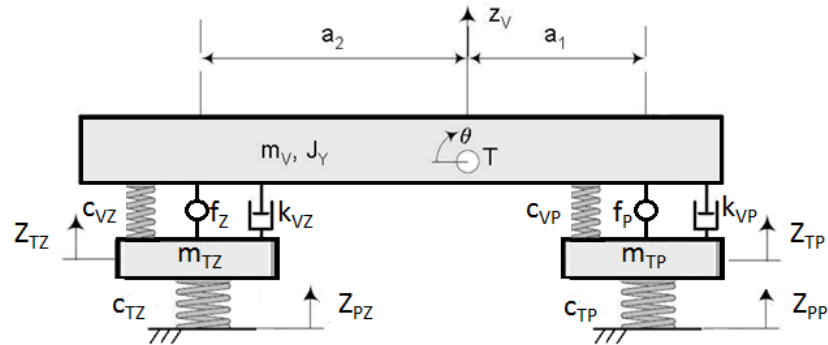


Figure 4. Two-dimensional oscillatory model with three masses

Equations which describe the given model are based on the conditions of dynamic balance presented with the following equations:

- Equation (5) illustrates the sum of all forces acting on sprung mass in  $z$ -axis direction:

$$m_V \frac{d^2 z_V}{dt^2} + k_{VP} \left( \frac{dz_V}{dt} - \frac{dz_{TP}}{dt} - a_1 \frac{d\theta}{dt} \right) + k_{VZ} \left( \frac{dz_V}{dt} - \frac{dz_{TZ}}{dt} + a_2 \frac{d\theta}{dt} \right) + c_{VP}(z_V - z_{TP} - a_1\theta) + c_{VZ}(z_V - z_{TZ} + a_2\theta) - f_P - f_Z = 0 \quad (5)$$

- Equation (6) illustrates the sum of all moments around  $y$ -axis:

$$J_Y \frac{d^2 \theta}{dt^2} + a_1 \cdot k_{VP} \left( \frac{dz_V}{dt} - \frac{dz_{TP}}{dt} - a_1 \frac{d\theta}{dt} \right) + a_2 \cdot k_{VZ} \left( \frac{dz_V}{dt} - \frac{dz_{TZ}}{dt} + a_2 \frac{d\theta}{dt} \right) - a_1 \cdot c_{VP}(z_V - z_{TP} - a_1\theta) + c_{VZ}(z_V - z_{TZ} + a_2\theta) + f_P a_1 - f_Z a_2 = 0 \quad (6)$$

- Equation (7) illustrates the sum of all forces acting on front unsprung mass in  $z$ -axis direction:

$$m_{TP} \frac{d^2 z_{TP}}{dt^2} - k_{VP} \left( \frac{dz_V}{dt} - \frac{dz_{TP}}{dt} - a_1 \frac{d\theta}{dt} \right) + c_{TP}(z_{TP} - z_{PP}) - c_{VP}(z_V - z_{TP} - a_1\theta) + f_P = 0 \quad (7)$$

- Equation (8) illustrates the sum of all forces acting on the rear unsprung mass in  $z$ -axis direction:

$$m_{TZ} \frac{d^2 z_{TZ}}{dt^2} - k_{VZ} \left( \frac{dz_V}{dt} - \frac{dz_{TZ}}{dt} + a_2 \frac{d\theta}{dt} \right) + c_{TZ}(z_{TZ} - z_{PZ}) - c_{VZ}(z_V - z_{TZ} - a_2\theta) + f_Z = 0 \quad (8)$$

### 3.3. Three-dimensional vehicle model

This model is also called the full vehicle model and it has seven degrees of freedom of movement. Seven degrees of freedom are represented by the vertical movement of sprung mass ( $m_V$ ) and four unsprung masses ( $m_{TP}$  and  $m_{TZ}$ ) in z-axis direction, as well as angular movements of vehicle around x and y axis, all of which describe this system. Three-dimensional vehicle model with five masses is presented in Figure 5.

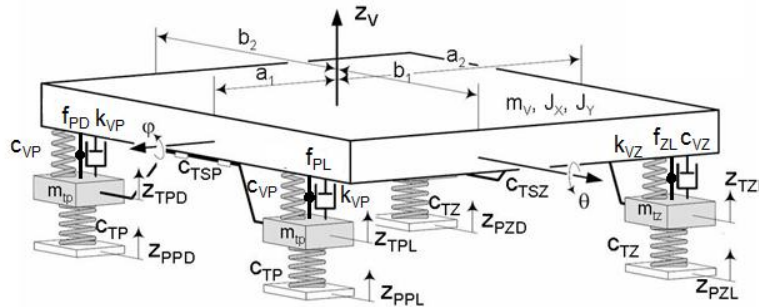


Figure 5. Three-dimensional oscillatory model with five masses

Equations which describe model presented in Figure 5, which were formed from the dynamic balance conditions, are as follows:

- Equation (9) illustrates the sum of all forces acting on sprung mass in z-axis direction:

$$\begin{aligned}
 m_V \frac{d^2 z_V}{dt^2} + k_{VP} \left( \frac{dz_V}{dt} - \frac{dz_{TPL}}{dt} + b_1 \frac{d\phi}{dt} - a_1 \frac{d\theta}{dt} \right) + k_{VP} \left( \frac{dz_V}{dt} - \frac{dz_{TPD}}{dt} - b_2 \frac{d\phi}{dt} - a_1 \frac{d\theta}{dt} \right) + \\
 + k_{VZ} \left( \frac{dz_V}{dt} - \frac{dz_{TZD}}{dt} - b_2 \frac{d\phi}{dt} + a_2 \frac{d\theta}{dt} \right) + k_{VZ} \left( \frac{dz_V}{dt} - \frac{dz_{TZL}}{dt} + b_1 \frac{d\phi}{dt} + a_2 \frac{d\theta}{dt} \right) + \\
 + c_{VP} (z_V - z_{TPL} + b_1 \phi - a_1 \theta) + c_{VP} (z_V - z_{TPD} - b_2 \phi - a_1 \theta) + \\
 + c_{VZ} (z_V - z_{TZD} - b_2 \phi + a_2 \theta) + c_{VZ} (z_V - z_{TZL} + b_1 \phi + a_2 \theta) - \\
 - f_{PL} - f_{PD} - f_{ZL} - f_{ZD} = 0
 \end{aligned} \tag{9}$$

- Equation (10) illustrates the sum of all moments around x-axis:

$$\begin{aligned}
 J_X \frac{d^2 \phi}{dt^2} + b_1 k_{VP} \left( \frac{dz_V}{dt} - \frac{dz_{TPL}}{dt} + b_1 \frac{d\phi}{dt} - a_1 \frac{d\theta}{dt} \right) - b_2 k_{VP} \left( \frac{dz_V}{dt} - \frac{dz_{TPD}}{dt} - b_2 \frac{d\phi}{dt} - a_1 \frac{d\theta}{dt} \right) - \\
 - b_2 k_{VZ} \left( \frac{dz_V}{dt} - \frac{dz_{TZD}}{dt} - b_2 \frac{d\phi}{dt} + a_2 \frac{d\theta}{dt} \right) + b_1 k_{VZ} \left( \frac{dz_V}{dt} - \frac{dz_{TZL}}{dt} + b_1 \frac{d\phi}{dt} + a_2 \frac{d\theta}{dt} \right) + \\
 + b_1 c_{VP} (z_V - z_{TPL} + b_1 \phi - a_1 \theta) - b_2 c_{VP} (z_V - z_{TPD} - b_2 \phi - a_1 \theta) - \\
 - b_2 c_{VZ} (z_V - z_{TZD} - b_2 \phi + a_2 \theta) + b_1 c_{VZ} (z_V - z_{TZL} + b_1 \phi + a_2 \theta) + c_{TS} \phi + \\
 + b_1 (f_{PL} + f_{ZL}) - b_2 (f_{PD} + f_{ZD}) = 0
 \end{aligned} \tag{10}$$

- Equation (11) illustrates the sum of all moments around y-axis:

$$\begin{aligned}
& J_y \frac{d^2 \theta}{dt^2} - a_1 k_{VP} \left( \frac{dz_V}{dt} - \frac{dz_{TPL}}{dt} + b_1 \frac{d\varphi}{dt} - a_1 \frac{d\theta}{dt} \right) - a_1 k_{VP} \left( \frac{dz_V}{dt} - \frac{dz_{TPD}}{dt} - b_2 \frac{d\varphi}{dt} - a_1 \frac{d\theta}{dt} \right) + \\
& + a_2 k_{VZ} \left( \frac{dz_V}{dt} - \frac{dz_{TZD}}{dt} - b_2 \frac{d\varphi}{dt} + a_2 \frac{d\theta}{dt} \right) + a_2 k_{VZ} \left( \frac{dz_V}{dt} - \frac{dz_{TZL}}{dt} + b_1 \frac{d\varphi}{dt} + a_2 \frac{d\theta}{dt} \right) + \\
& - a_1 c_{VP} (z_V - z_{TPL} + b_1 \varphi - a_1 \theta) - a_1 c_{VP} (z_V - z_{TPD} - b_2 \varphi - a_1 \theta) + \\
& + a_2 c_{VZ} (z_V - z_{TZD} - b_2 \varphi + a_2 \theta) + a_2 c_{VZ} (z_V - z_{TZL} + b_1 \varphi + a_2 \theta) + \\
& + a_2 (f_{ZL} + f_{ZD}) - a_1 (f_{PL} + f_{PD}) = 0
\end{aligned} \tag{11}$$

– Equation (12) illustrates the sum of all forces acting on front left unsprung mass in  $z$ -axis direction:

$$\begin{aligned}
& m_{TP} \frac{d^2 z_{TPL}}{dt^2} - k_{VP} \left( \frac{dz_V}{dt} - \frac{dz_{TPL}}{dt} + b_1 \frac{d\varphi}{dt} - a_1 \frac{d\theta}{dt} \right) - c_{VP} (z_V - z_{TPL} + b_1 \varphi - a_1 \theta) - \\
& - c_{TS} \frac{\varphi}{b_1 + b_2} + c_{TP} (z_{TPL} - z_{PPL}) + f_{PL} = 0
\end{aligned} \tag{12}$$

– Equation (13) illustrates the sum of all forces acting on front right unsprung mass in  $z$ -axis direction:

$$\begin{aligned}
& m_{TP} \frac{d^2 z_{TPD}}{dt^2} - k_{VP} \left( \frac{dz_V}{dt} - \frac{dz_{TPD}}{dt} - b_2 \frac{d\varphi}{dt} - a_1 \frac{d\theta}{dt} \right) - c_{VP} (z_V - z_{TPD} - b_2 \varphi - a_1 \theta) + \\
& + c_{TS} \frac{\varphi}{b_1 + b_2} + c_{TP} (z_{TPD} - z_{PPD}) + f_{PD} = 0
\end{aligned} \tag{13}$$

– Equation (14) illustrates the sum of all forces acting on rear right unsprung mass in  $z$ -axis direction:

$$\begin{aligned}
& m_{TZ} \frac{d^2 z_{TZD}}{dt^2} - k_{VZ} \left( \frac{dz_V}{dt} - \frac{dz_{TZD}}{dt} - b_2 \frac{d\varphi}{dt} - a_2 \frac{d\theta}{dt} \right) - \\
& - c_{VZ} (z_V - z_{TZD} - b_2 \varphi + a_2 \theta) + c_{TZ} (z_{TZD} - z_{PZD}) + f_{ZD} = 0
\end{aligned} \tag{14}$$

– Equation (15) illustrates the sum of all forces acting on rear left unsprung mass in  $z$ -axis direction:

$$\begin{aligned}
& m_{TZ} \frac{d^2 z_{TZL}}{dt^2} - k_{VZ} \left( \frac{dz_V}{dt} - \frac{dz_{TZL}}{dt} + b_1 \frac{d\varphi}{dt} + a_2 \frac{d\theta}{dt} \right) - \\
& - c_{VZ} (z_V - z_{TZL} + b_1 \varphi + a_2 \theta) + c_{TZ} (z_{TZL} - z_{PZL}) + f_{ZL} = 0
\end{aligned} \tag{15}$$

#### 4. Setting PID regulator coefficients

There are several methods for adjusting the coefficients of the PID controller, which can be seen in [9]. However, when the coefficients of the PID controller are adjusted in Simulink, it is possible to perform automatic adjustments. Figure 6. shows this way of setting the PID controller in Simulink.

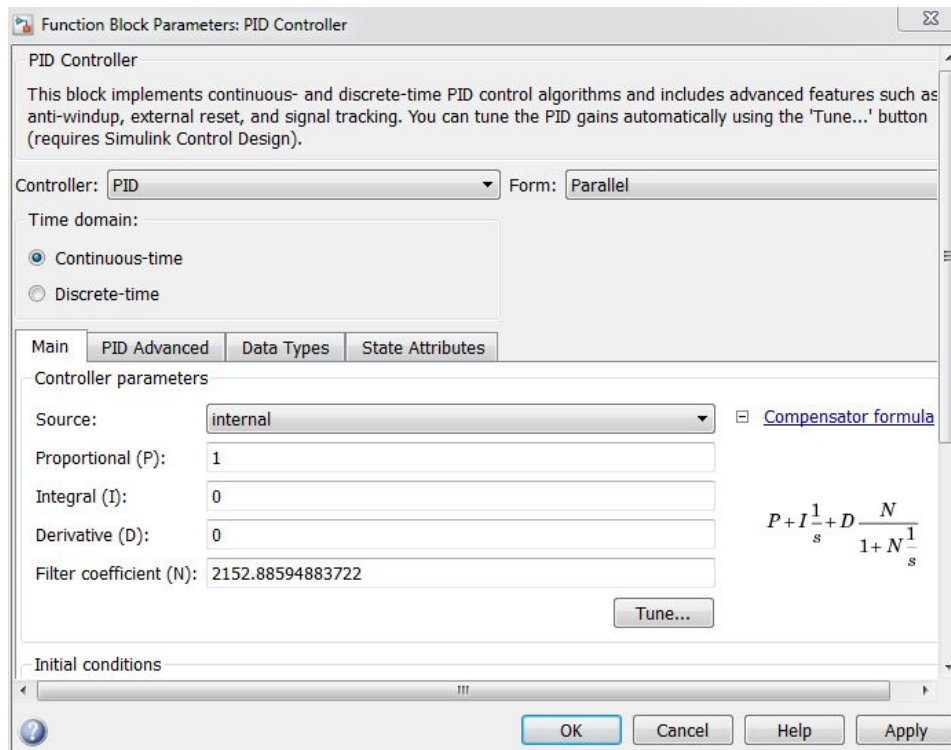


Figure 6. Adjustment of PID controller parameters

At the very beginning, it is necessary to enter arbitrary values for the parameters (P), (I) and (D). After that, the button *Tune* is clicked, and the form like the one in Figure 7. is shown.

Figure 7. shows the appearance of a signal to be adjusted, with default values from Figure 6. (dashed line) and the appearance of the signal after the adjustment. The values of the parameters (P), (I) and (D) can be seen in the lower right corner. This appearance of the signal is automatically offered to the programme user who can change its appearance. This is achieved by moving the slider *Response Time* and *Transient Behavior*.

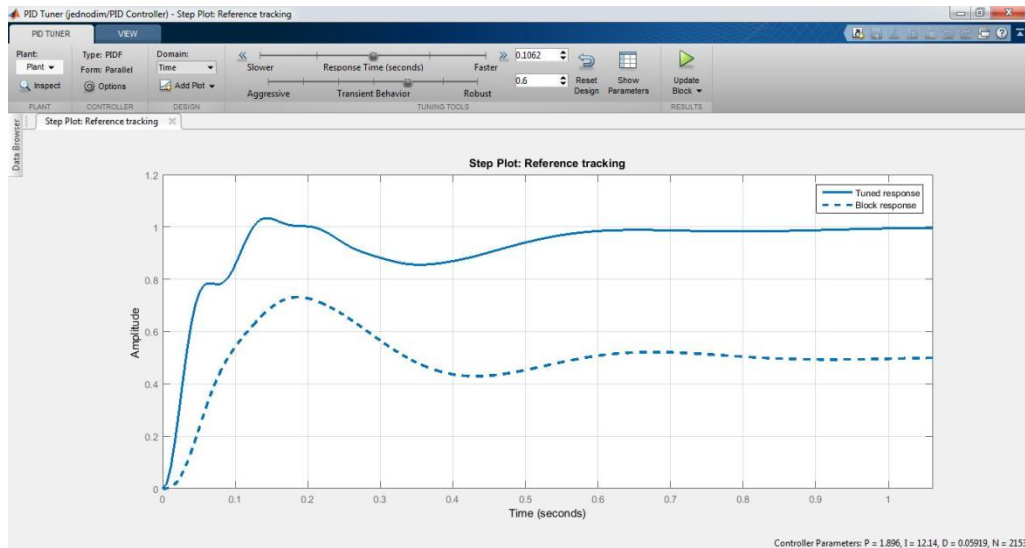


Figure 7. The form for optimization of PID controller parameters

Once the satisfactory values of controller parameters are obtained, the button *Update Block* should be clicked, and then the new parameters are automatically entered into the appropriate fields, as seen in Figure 8. After which the Simulink model can be started and further analysis of the problem can be continued.

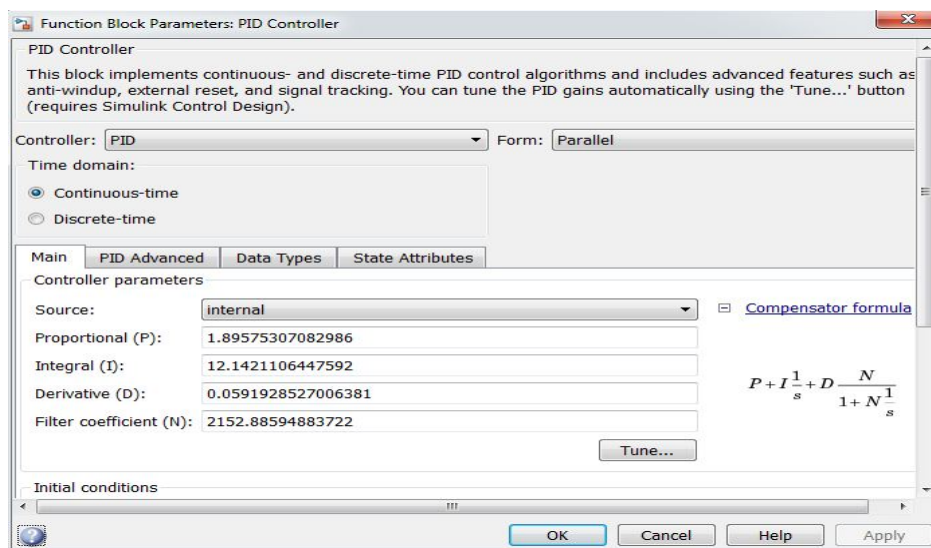


Figure 8. PID controller parameters after adjustment

If the model created in Simulink is correct, there will be no need for additional adjustments, as this block will automatically adjust (P), (I) and (D) parameters to optimal values.

## 5. Simulation and results

Simulation and analysis of the results are carried out for the vehicle models presented in Section 3. Values of certain parameters of the vehicle and suspension system are given in Table 1.

Characteristics of vehicles for the masses and the position of center of gravity in Table 1. are obtained by references in [10]. The data for radius of inertia around the x-axis and y are obtained by references in [11]. In the equations, figures (6), (10) and (11)  $J_X$  and  $J_Y$  are determined according to the literature [11].

$$J_X = m_V \cdot i_X^2 = 409,6 \text{ kgm}^2, J_Y = m_V \cdot i_Y^2 = 1277 \text{ kgm}^2 \quad (16)$$

The remaining parameters of the suspension system are obtained from empirical research.

The following section provides diagrams of oscillatory behavior of sprung mass and unsprung mass of the vehicle for all three models. Each diagram shows a comparison between passive and active suspension system. In order to prevent repetition of results and maintain their consistency during presentation of results, only some of the results of oscillatory behavior are shown for each respective model in order to provide a clearer comparison of passive and active suspension systems.

Figures 9., 10. and 11. show comparative diagrams of vertical movement, velocity and acceleration of sprung mass for  $\frac{1}{4}$  vehicle model for case of passive and active suspension system. Road profile is defined as a trapezoidal obstacle on the road.

It can be seen from Figures 9., 10. and 11. that with the active suspension applied to  $\frac{1}{4}$  vehicle model, a decrease in amplitude and period of oscillation occurs.

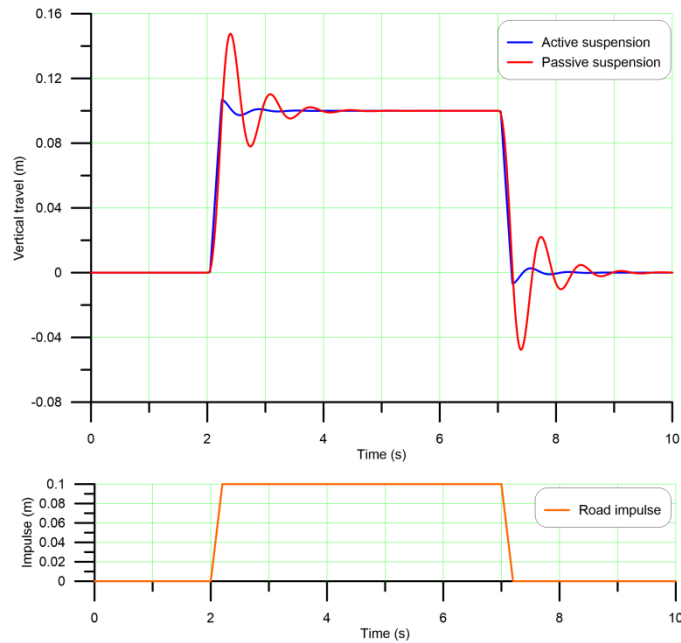


Figure 9. Vertical travel of sprung mass  $m_v$

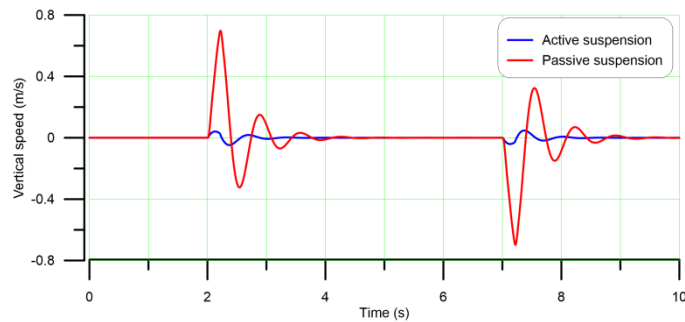


Figure 10. Sprung mass  $m_v$  vertical travel speed

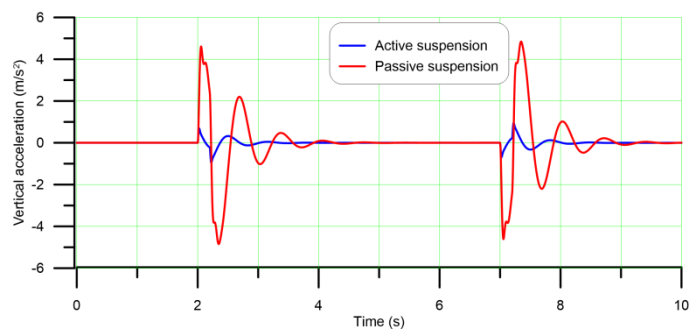


Figure 11. Sprung mass  $m_v$  vertical travel acceleration

Figure 12. shows vertical travel of the wheels (unsprung mass) in two-dimensional oscillatory models in case of passive and active suspension systems. In this case, the impulse in the system is represented by two obstacles on the road in the form of a square.

It can be seen from Figure 12. that the regulation of suspension using a PID controller reduces the amplitude and period of oscillations as well as the vertical movement of unsprung mass (wheel) of vehicle.

In order to analyse what happens to the sprung mass during vehicle movement, Figures 13., 14. and 15. show the angle of rotation, angular velocity and angular acceleration of rotation of the sprung mass around the y-axis.

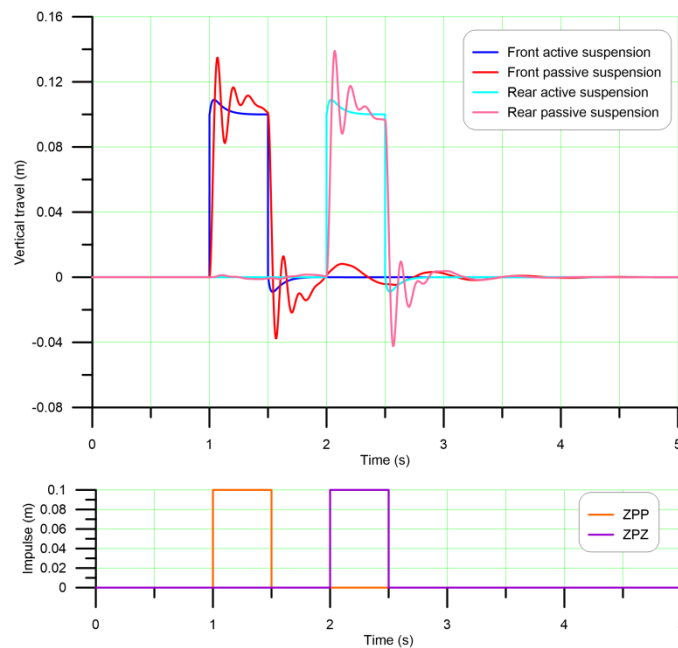


Figure 12. *Two-dimensional model vertical travel of unprung masses*

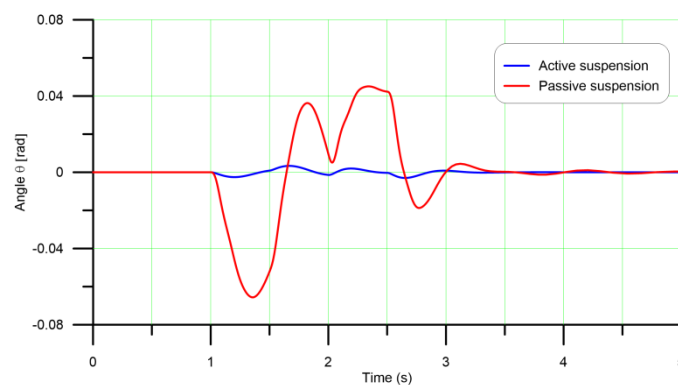


Figure 13. *Rotation angle of sprung mass( $m_v$ ) around y-axis*

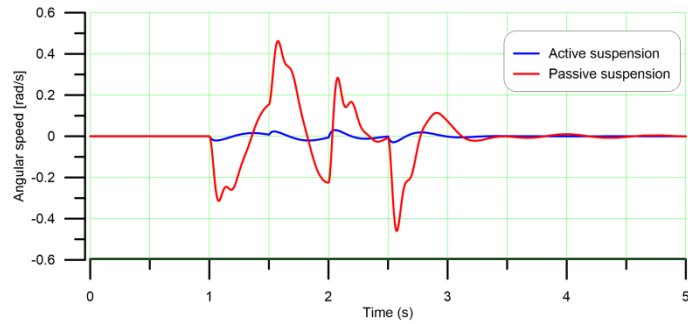


Figure 14. Angular speed of sprung mass ( $m_v$ ) around y-axis

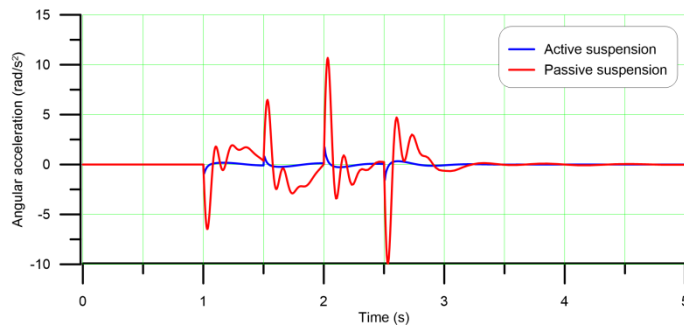


Figure 15. Angular acceleration of sprung mass ( $m_v$ ) around y-axis

It can be seen from Figures 13., 14., and 15. that by applying PID controller with this oscillatory model a reduction of the amplitude of oscillation for sprung mass  $m_v$  was achieved.

Table 1. – Vehicle characteristics

Description	Label	Value
<b>One-dimensional vehicle model</b>		
Sprung mass	$m_v$	250 kg
Unsprung mass	$m_T$	30 kg
Suspension system stiffness	$c_v$	25000 N/m
Tire stiffness	$c_T$	145000 N/m
Suspension system damping	$k_v$	2200 Ns/m
<b>Two-dimensional vehicle model</b>		
Sprung mass	$m_v$	500 kg

Front unsprung mass	$m_{TP}$	60 kg
Rear unsprung mass	$m_{TZ}$	60 kg
Front and rear suspension system stiffness	$c_{VP}=c_{VZ}$	25000 N/m
Front and rear tire stiffness	$c_{TP}=c_{TZ}$	145000 N/m
Front and rear suspension system damping	$k_{VP}=k_{VZ}$	1500 Ns/m
Radius of inertia around y-axis	$i_Y$	1,13 m
Vehicle centre of gravity in longitudinal plane	$a_1$	0,933 m
	$a_2$	1,557 m
<b>Three-dimensional vehicle model</b>		
Sprung mass	$m_V$	1000 kg
Front left and right unsprung mass	$m_{TPL}=m_{TPD}$	30 kg
Rear left and right unsprung mass	$m_{TZL}=m_{TZD}$	30 kg
Front and rear suspension system stiffness	$c_{VP}=c_{VZ}$	25000 N/m
Front and rear tire stiffness	$c_{TP}=c_{TZ}$	145000 N/m
Torsion stabilizer stiffness	$c_{TS}$	45000 N/m
Front and rear suspension system damping	$k_{VP}=k_{VZ}$	1500 Ns/m
Radius of inertia around x-axis	$i_X$	0,64 m
Radius of inertia around y-axis	$i_Y$	1,13 m
Vehicle centre of gravity in longitudinal plane	$a_1$	0,933 m
	$a_2$	1,557 m
Vehicle center of gravity in transverse plane	$b_1$	0,706 m
	$b_2$	0,706 m

Results of the simulations of passive and active oscillatory model of a full vehicle are provided next. Road profile which the vehicle is moving on is defined in Figure 16.

Analysis of the change of angle rotations of sprung mass around  $x$ -axis (angle  $\alpha$ ) and around  $y$ -axis (angle  $\beta$ ) was performed. Results were presented in Figures 17. and 18.

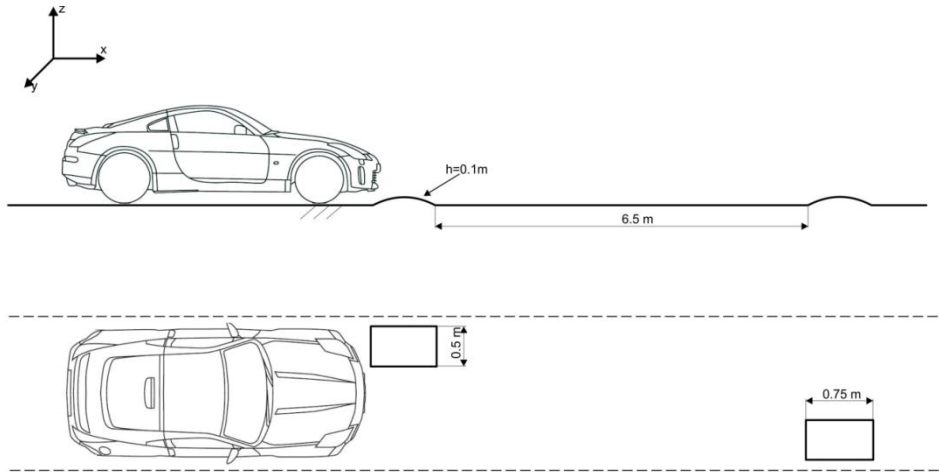


Figure 16. Road profile to be used in three-dimensional model analysis

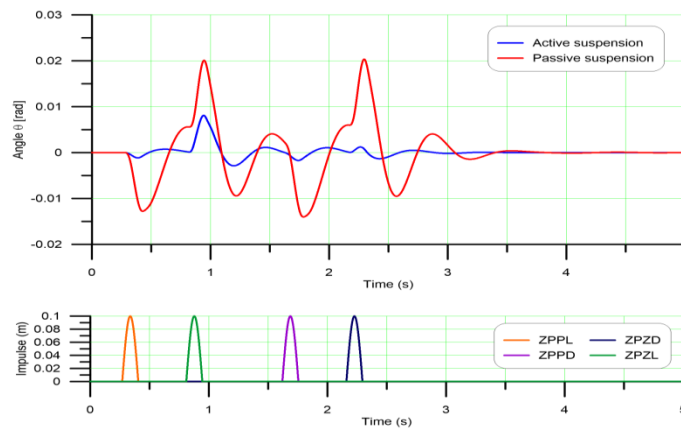


Figure 17. Rotation angle of sprung mass ( $m_v$ ) around  $x$ -axis

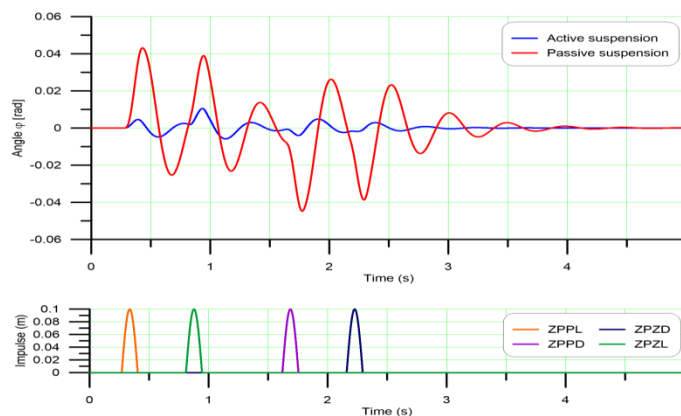


Figure 18. Rotation angle of sprung mass ( $m_v$ ) around  $y$ -axis

Figures 17. and 18. show that by applying PID controller with oscillatory model of full vehicle the amplitude of oscillation of sprung mass around randy axis of the analysed model was decreased, and settling time is faster, too.

## 6. Conclusion

Analysis of oscillatory models of vehicles carried out in this paper has shown that the mathematical models that describe the oscillatory passive suspension systems can be easily modified, so as to describe the models with active suspension systems. Three oscillatory models, described herein, have included PID controller as an element of regulation which is installed between sprung mass and unsprung mass.

It is shown that by using block of PID controller in Simulink program automatic adjustment of parameters of PID controller can be performed. Thus avoiding the complicated setting the parameters of the PID controller by methods available in the literature. Automatically set values of parameters of PID controller have shown in the analysis of oscillatory behavior of certain parameters in oscillating models the justification of use of this type of controller for modeling active suspension system of vehicles.

## References

- [1] Bin Nawawi,Zulkifli.“Vibration investigation for passenger car with different damping characteristic on car suspension systems”, *Faculty of Mechanical Engineering Universiti Malaysia Pahang, B.Sc. Thesis*, 2012
- [2] Šehović, Jasmin and Pikula, Boran.“Analysis of effects of vehicle suspension system stiffness and damping on oscillatory comfort”, *International Journal of Engineering & Scientific Research*, Volume 3, Issue 12, 2015
- [3] Lajqi,Shpetim andPehan, Stanislav.“Designs and Optimizations of Active and Semi-Active Non-linear Suspension Systems for a Terrain Vehicle”, *Strojnikivestnik - Journal of Mechanical Engineering* 58(2012)12, 732-743, 2012
- [4] Tameshwer,Nath andRastogi,Vikas.“Quarter/Half/Full Car Models for Active Suspension (with PID controller)”, *International conference on Recent Trends in Engineering &Technology*, 2012

- [5] Choudhury, SoudFarhan anddr. M. A. Sarkar, Rashid.“An approach on performance comparison between automotive passive suspension and active suspension system (PID controller) using Matlab/Simulink”, *Journal of Theoretical and Applied Information Technology*, vol. 43, no. 2, 2012
- [6] Katal,Nitish and Kr. Singh, Sanjay.“Optimization of PID Controller for Quarter-Car Suspension System using Genetic Algorithm”, *International Journal of Advanced Research in Computer Engineering & Technology (IJARCET)* Volume 1, Issue 7, 2012
- [7] Tehrani, Kambiz Arab and Mpanda, Augustin.,PIDControl Theory, Introduction to PID Controllers -Theory, Tuning and Application to Frontier Areas“, *Prof. Rames C. Panda (Ed.)*, ISBN: 978-953-307-927-1, 2012
- [8] Kunya, Abdullahi B. and Ata, Atef A. “Half car suspension system integrated with PID controller”, *Proceedings 29th European Conference on Modelling and Simulation ©ECMS*, ISBN: 978-0-9932440-0-1, 2015
- [9] Kuyvenhoven, Neil.“PID Tuning Methods; An Automatic PID Tuning Study with MathCad”, *Calvin College*, 2012
- [10] Westrup, K., “Der dritte Mann”, *Auto Motor und Sport*, Heft 19/2000, pp 36-41, 2000
- [11] Jazar, Reza.“Vehicle Dynamics Theory and Application”, *Springer science+Business media, LLC, New York*, 2008

## Nomenclature

Label	Unit	Description
$a_1, a_2$	[m]	Coordinates of vehicle gravity center in vehicle longitudinal plane
$b_1, b_2$	[m]	Coordinates of vehicle gravity center in vehicle transverse plane
$c_T$	[N/m]	Tire stiffness
$c_{TP}$	[N/m]	Front tire stiffness
$c_{TS}$	[N/m]	Torsion stabilizer stiffness
$c_{TZ}$	[N/m]	Rear tire stiffness
$c_V$	[N/m]	Suspension system stiffness
$c_{VP}$	[N/m]	Front suspension system stiffness
$c_{VZ}$	[N/m]	Rear suspension system stiffness
$f$	[N]	Active force in suspension system regulation

$f_P$	[N]	Active force in front suspension system regulation
$f_{PD}$	[N]	Active force in front right suspension system regulation
$f_{PL}$	[N]	Active force in front left suspension system regulation
$F_x$	[N]	Sum of all forces acting on a vehicle in x-axis direction
$F_y$	[N]	Sum of all forces acting on a vehicle in y-axis direction
$F_z$	[N]	Sum of all forces acting on a vehicle in z-axis direction
$f_Z$	[N]	Active force in rear suspension system regulation
$f_{ZD}$	[N]	Active force in rear right suspension system regulation
$f_{ZL}$	[N]	Active force in rear left suspension system regulation
$i_x$	[m]	Radius of inertia around x-axis
$i_y$	[m]	Radius of inertia around y-axis
$J_x$	[kgm <sup>2</sup> ]	Moment of inertia of sprung mass around x-axis
$J_y$	[kgm <sup>2</sup> ]	Moment of inertia of sprung mass around y-axis
$K_p$		Proportional coefficient of PID regulator
$k_v$	[Ns/m]	Suspension system damping
$k_{vP}$	[Ns/m]	Front suspension system damping
$k_{vZ}$	[Ns/m]	Rear suspension system damping
$m_T$	[kg]	Mass of unsprung mass
$m_{TP}$	[kg]	Mass of front unsprung mass
$m_{TZ}$	[kg]	Mass of rear unsprung mass
$m_v$	[kg]	Mass of sprung mass
$M_x$	[Nm]	Sum of all moments acting on a vehicle around x-axis
$M_y$	[Nm]	Sum of all moments acting on a vehicle around y-axis
$M_z$	[Nm]	Sum of all moments acting on a vehicle around z-axis
$T_d$		Derivative coefficient of PID regulator
$T_i$		Integral coefficient of PID regulator
$z_P$	[m]	Impulse from the road
$z_{PP}$	[m]	Impulse from the road acting on a vehicle front axle
$z_{PPD}$	[m]	Impulse from the road acting on a vehicle front right wheel
$z_{PPL}$	[m]	Impulse from the road acting on a vehicle front left wheel
$z_{PZ}$	[m]	Impulse from the road acting on a vehicle rear axle

$z_{PZD}$	[m]	Impulse from the road acting on a vehicle rear right wheel
$z_{PZL}$	[m]	Impulse from the road acting on a vehicle rear left wheel
$z_T$	[m]	Travel of unsprung mass in z-axis direction
$z_{TP}$	[m]	Travel of front unsprung mass in z-axis direction
$z_{TPD}$	[m]	Travel of front right unsprung mass in z-axis direction
$z_{TPL}$	[m]	Travel of front left unsprung mass in z-axis direction
$z_{TZ}$	[m]	Travel of rear unsprung mass in z-axis direction
$z_{TZD}$	[m]	Travel of rear right unsprung mass in z-axis direction
$z_{TZL}$	[m]	Travel of rear left unsprung mass in z-axis direction
$z_V$	[m]	Travel of sprung mass in z-axis direction
$\phi_x$	[rad]	Angle of rotation of sprung mass around x-axis
$\phi_y$	[rad]	Angle of rotation of sprung mass around y-axis
$\phi_z$	[rad]	Angle of rotation of sprung mass around z-axis